Benchmark experiment on slab ^{238}U with D-T neutrons for validation of evaluated nuclear data

Yan-Yan Ding[1], Yang-Bo Nie[1,2,*], Yue Zhang[1], Zhi-Jie Hu[3], Qi Zhao[1], Huan-Yu Zhang[1], Kuo-Zhi Xu[1], Shi-Yu Zhang[1,2]， Xin-Yi Pan[1], Chang-Lin Lan[2], Jie Ren[1], Xi-Chao Ruan[1,2]

[1]Key Laboratory of Nuclear Data, China Institute of Atomic Energy, Beijing 102413, China

[2]School of Nuclear Science and Technology, Lanzhou University, Lanzhou 730000, China

[3]Institute of Fluid Physics, China Academy of Engineering Physics, Mianyang 62100, China

[*]Corresponding author.*E-mail Address:* nieyb@163.com

Abstract:

A benchmark experiment on ^{238}U slab samples was conducted using a deuterium–tritium neutron source at the China Institute of Atomic Energy. The leakage neutron spectra within energy levels of 0.8–16 MeV at 60° and 120° were measured using the time-of-flight method. The samples were prepared as rectangular slabs with a 30 cm square base and thicknesses of 3, 6, and 9 cm. The leakage neutron spectra were also calculated using the MCNP-4C program based on the latest evaluated files of ^{238}U evaluated neutron data from CENDL-3.2, ENDF/B-VIII.0, JENDL-5.0, and JEFF-3.3. Based on the comparison, the deficiencies and improvements in ^{238}U evaluated nuclear data were analyzed. The results showed the following. (1) The calculated results for CENDL-3.2 significantly overestimated the measurements in the energy interval of elastic scattering at 60° and 120°. (2) The calculated results of CENDL-3.2 overestimated the measurements in the energy interval of inelastic scattering at 120°. (3) The calculated results for CENDL-3.2 significantly overestimated the measurements in the 3–8.5MeV energy interval at 60° and 120°. (4) The calculated results with JENDL-5.0 were generally consistent with the measurement results.

Key words: leakage neutron spectra; uranium; D-T neutron source; evaluated nuclear data.

1. Introduction

Nuclear data are widely used in almost all important fields of nuclear science and technology, such as nuclear power, nuclear medicine, and nuclear safety, and they are the link between basic research in nuclear physics and the application of nuclear technology[1-5]. The accuracy, integrity, and reliability of nuclear data influences the development of the nuclear industry[6,7]. A benchmark experiment is an integral measurement of the parameters that can be presented with a few approximations and assumptions. This method is effective for verifying the accuracy of nuclear data [8-10]. The objective of this approach is to determine the differences and deficiencies between the measurements and predictions of different evaluated neutron libraries. The discrepancies between the measurements and calculations can guide the evaluator to flexibly adjust the parameters that influence the calculated cross-section.

Uranium is a radioactive nuclide that contains three natural isotopes (^{238}U, ^{235}U, and ^{234}U). The natural abundance of ^{238}U is 99.27%, which is the highest among the three isotopes. Advanced

nuclear energy systems, such as the fusion–fission hybrid reactor[11,12], accelerator-driven system[13,14] and fast reactor[15], have the ability to breed nuclear fuel and transmute waste, and ^{238}U plays a crucial role in emitting relatively fast neutrons in these processes. ^{238}U has been one of the most significant components of the nuclear fuel cycle, including fuel enrichment facilities, power reactors, and spent fuel storage, and it constitutes more than 90% of the fuel in power reactors[16,17]. The Collaborative International Evaluated Library Organization of the Organization for Economic Co-operation and Development Nuclear Energy Agency, an international organization that evaluates nuclear data, first focused on identifying discrepancies in the evaluation of a few high-priority isotopes, including ^{238}U[18]. A series of measurements are being planned at the neutron time-of-flight (TOF) facility of the European Council for Nuclear Research and the Geel Electron Linear Accelerator TOF facility at the Institute for Reference Materials and Measurements[19].With rapid advancements in nuclear technology, more accurate nuclear data of ^{238}U are required.

The international evaluated databases all contained neutron data for ^{238}U, and we investigated the evaluation of the CENDL-3.2 [20], ENDF/B-VIII.0 [21], JENDL-5.0 [22], and JEFF-3.3 [23] libraries. Table 1 lists the evaluated information for the ^{238}U neutron data from the four libraries. The data type of ^{238}U in the four libraries included cross-sections of various reactions, angular distributions, and double differential spectra. All other libraries, except CENDL-3.2, contained covariance information.

Table 1 Evaluated data of n+^{238}U reaction

Library	CENDL-3.2	ENDF/B-VIII.0	JENDL-5.0	JEFF-3.3
Evaluation time	EVAL-MAY19	EVAL-DEC14	EVAL-NOV09	EVAL-MAR17
Author	G. Y. Tang, Z. M. Shi, B. S. Yu, G. C. Chen	IAEA Consortium	O. Iwamoto, N. Otuka, S. Chiba	CEA/DAM-DEN EC-JRC Geel COLL.
Energy range	20 MeV	30 MeV	200 MeV	30 MeV
Calculation code	FUNF03[a]	EMPIRE-3.2.3	CCONE	TALYS

[a]The FUNF code can analyze a set of neutron nuclear data with incident energies ranging from 1 keV to 20 MeV, including cross-sections of all reaction channels, angular-energy distributions of emitted neutrons, double-differential cross-sections of various emitted secondary particles, and gamma production: multiplicity, cross-section, angular distribution, energy spectrum, etc.

Most neutron data of ^{238}U in the CENDL-3.2 library were evaluated in 1990, when FMT was adopted as the main code, and the theoretical model of this code has not been reported publicly. Subsequent updates mainly included the following: (1) In 2004, the angular distribution of secondary neutrons and gamma production were replaced with calculations based on the FUNF03 code[24]. The contributions of direct inelastic scattering were replaced with the calculated results based on the ECIS95[25] and DWUCK4[26] codes. (2) The gamma production spectrum was revised in 2008. (3) In 2009, the energy and angular distributions of secondary neutrons from inelastic continuum scattering were replaced with results calculated using the FUNF03 code. (4) In 2019, the delayed gamma data were evaluated and compiled again, and the resonance parameters were adopted from the ENDF/B-VII.1 data file.

A few experiments have been conducted on ^{238}U to identify discrepancies in the evaluation of ^{238}U with D-T neutrons. In 1979, the leakage neutron and gamma spectra from ^{238}U spherical shells with different radii were measured by Lusia F. Hansen at Lawrence Livermore National Laboratory[27]; In 2010, Y. Nie performed leakage neutron spectra measurements on a ^{238}U sample (a 10 cm square base with a 5 cm thickness) using D-T neutron source at the integral experimental facility in the China Institute of Atomic Energy (CIAE), at measured angles of 45° and 135°[28]. Subsequently, in 2016, new measurements were performed at 60° and 120° on ^{238}U samples with geometric dimensions of 10 cm square area and 2, 5, and 11 cm thicknesses[29].

In this study, three larger ^{238}U samples were used to improve the count rate of leaked neutrons and obtain more accurate experimental data. The experimental samples were shaped as rectangular slabs with a square base of 30 cm and thicknesses of 3, 6, and 9 cm, corresponding to 0.81, 1.62, and 2.43 mpfs, respectively, for a 14.5 MeV neutron. During the TOF measurements, neutrons leaking from the rectangular slabs were measured using a BC-501A detector at measurement angles of 60° and 120° from energy intervals between 0.8 and 16 MeV, using pulsed D-T neutrons. The results were analyzed to examine the ^{238}U data files of CENDL-3.2, ENDF/B-VIII.0, JENDL-5.0, and JEFF-3.3. A Monte Carlo code, MCNP-4C[30], was used to perform the measurements.

2. Experimental Setup

The measurements were conducted at a benchmark experimental facility built on the pulsed neutron generator of the CIAE. A series of measurements on the slab samples have been previously performed at this facility[31-34]. Fig.1 shows the layout of the experimental setup.

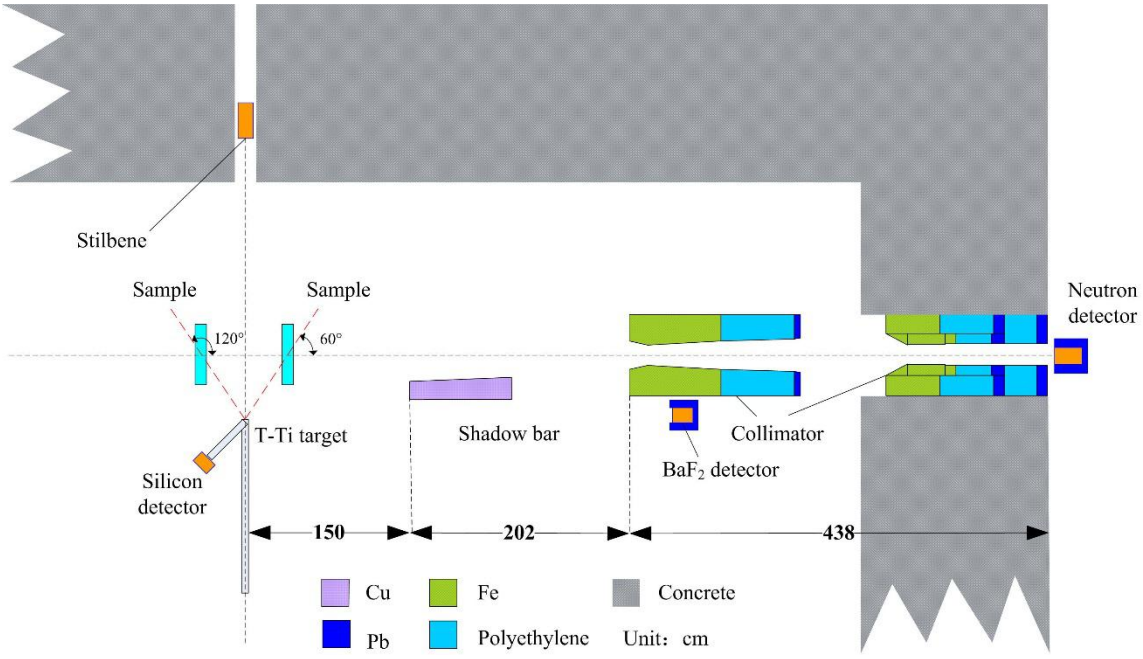

Fig.1 Schematic for measurements of leakage neutron at CIAE.

2.1 Neutron source

The neutron source was produced using a 400 kV Cockcroft–Walton accelerator at CIAE, which were generated at the tritium–titanium (T-Ti) target with a surface density of 1.2 mg/cm^2 via bombardment of a pulsed deuteron (D^+) beam. During the experiment, the energy and average current were 300 keV and 20 μA, respectively, at a repetition rate of 1.5 MHz. The neutron pulse width was as narrow as approximately 2ns. The energy of the pulsed neutrons was approximately

14.5 MeV, with a yield of 2×10^9 n/s at the target. An associated particle system at 135° was established to measure the yield of the neutrons, which majorly included a silicon surface-barrier detector (SSD). Although neutrons are produced through the T (d, n)^{4}He reaction, alpha particles are produced at the reverse angle. The silicon detector was used to measure alpha particles in the $\Delta\Omega$ solid angle at angle φ to the incident D^+ beam, and $\phi_n(\theta, E_d)$ is the neutron flux in the unit solid angle at angle θ to the incident D^+ beam. These parameters can be calculated using Eqs. (2) and (3)[35,36]:

$$\phi_n(\theta, E_d) = \frac{N_\alpha}{\Delta\Omega} \times A_\alpha \qquad (1)$$

$$\Delta\Omega = \frac{\pi \times r^2}{L^2} \qquad (2)$$

where E_d is the average energy of deuteron ions participating in the reaction to produce neutrons in the T-Ti target, N_α is the count of alpha particles measured at angle φ, A_α is the corrective factor related to the energy of the D^+ beam and the emission angle of α particles. $\Delta\Omega$ is the solid angle of the silicon detector subtending the T-Ti target, r is the radius of the aperture to limit the solid angle in front of the silicon detector, and L is the distance between the aperture and the target.

The relationship between the neutron flux in the unit solid angle at angles θ, $\phi_n(\theta, E_d)$, expressed by Eq. (1), and the neutron yield is expressed as follows:

$$\frac{\phi_n(\theta)}{N_n} = \frac{\sigma(\theta)}{\sigma_{tot}} \qquad (3)$$

where σ_{tot} is the total cross-section of the D-T reaction, $\sigma(\theta)$ is the differential cross-section of the D-T reaction at angle θ. By substituting Eq. (1) into Eq. (3), the yield of neutrons can be obtained using Eq. (4):

$$N_n = \frac{N_\alpha \times A_\alpha \times \sigma_{tot}}{\Delta\Omega \times \sigma(\theta)} \qquad (4)$$

Here, the energy of the D^+ beam was approximately 300 keV, and E_d was approximately 147 keV. The alpha particles were measured at 135° ($\varphi = 135°$).When the neutron was emitted at 0° ($\theta = 0°$), σ_{tot} was 3984 mb, $\sigma(\theta)$ was 336 mb/sr, and A_α was assumed to be 1.263. The radius of the aperture was approximately 0.16 cm, and the distance between the limiting aperture and T-Ti target was approximately 90 cm. The expression, $N_n = N_\alpha \times 1.508\times10^6$, can be obtained. Therefore, as long as the number of ^{4}He particles is accurately measured, it is logical to calculate the number of neutrons.

2.2 Samples

The slab samples used in the experiment included one polyethylene sample and three ^{238}U samples. Polyethylene was used as a standard sample to test the reliability of the system; its purity was higher than 99.9%.The purity of the ^{238}U sample was higher than 99.37%. Further descriptions of the ^{238}U samples are provided in Table 2.

Table 2 Size, density, and composition of ^{238}U samples

Sample	Size(cm)	Density(g/cm^3)	Nuclide(mass ratio)
^{238}U	30×30×3	18.654	^{238}U(99.3770), ^{235}U(0.2015), C(0.159), N(0.019), Mo+Zn+Pb+Bi+Ta+Cd+Ni+Fe+Co+W+B+Si+Mn+Cr +Mg+Sn+V+Ca+Cu+Al(0.2486)
	30×30×6	18.649	
	30×30×9	18.868	

2.3 Collimator

During the experiment, neutrons interacted not only with the ^{238}U sample, but also with other devices in the laboratory. These neutrons entered the detector after scattering and forming background counts. Shields and collimators were used in the experiment to minimize the influence of the background and scattered neutrons on the experimental results[37]. As shown in Fig.1, a precollimator consisting of iron, polyethylene, and lead was set between the experimental sample and concrete wall along the flight path of the neutrons. The other collimator was placed inside a 2-m-thick concrete wall made of the same materials as the precollimator. A shadow bar was placed between the experimental sample and the precollimator along the flight path of the neutrons to eliminate the scattered background neutrons generated during the interaction between the source and the collimator. By using the shadow bar, precollimator, and wall collimator, the background spectrum (sample-out) measured during the experiment was significantly lower than the effect spectrum (sample-in), and the foreground–background ratio increased significantly (Fig.2).

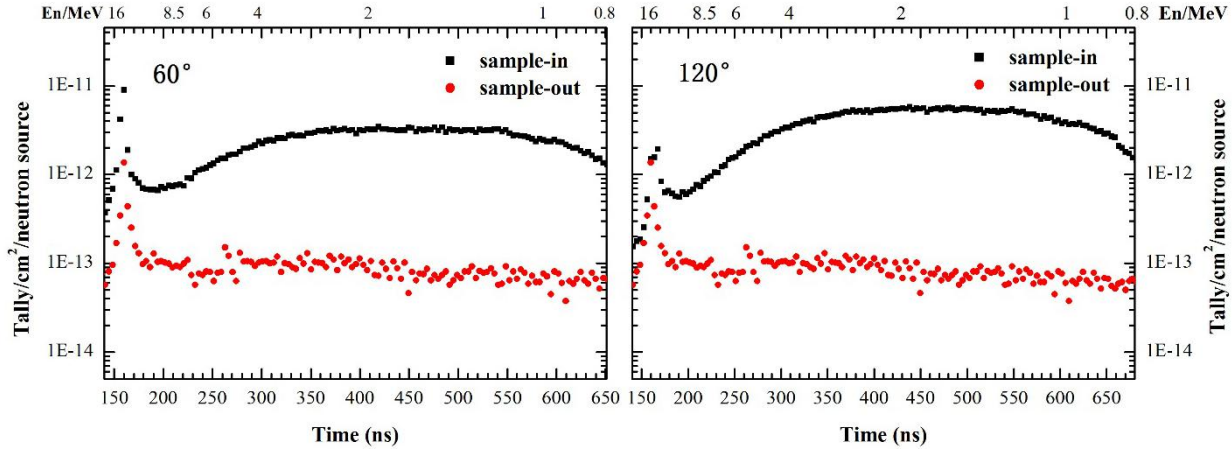

Fig.2 TOF measurement results at 60° and 120° under sample-in and sample-out conditions.

2.4 Electronics system and data processing

A simplified diagram of the measurement circuit is shown in Fig.3. The leakage neutron spectra measurements were conducted using a scintillation detector comprising a BC-501A scintillator with a diameter and thickness of 5.08 and 2.54 cm, respectively. The BC-501Asignal was divided into two outputs. One output entered the analog-to-digital converter as the pulse height (PH), and the other was used to determine the TOF and pulse shape discrimination (PSD). The TOF was derived by considering the anode signal as the start-time signal, and the beam pick-up signal from the accelerator was used as the stop signal after an appropriate delay. The PH was used for energy calibration to determine the detector threshold. The PSD was used for n-γ discrimination to eliminate γ-ray events.

Stilbene and BaF_2 scintillation crystals were used to detect the TOF spectra of the source neutrons and TOF spectra of associated gamma rays, respectively. After adequate processing of these spectra, the time distribution of the pulsed neutrons was obtained. The SSD signal was the

output of the silicon detector and was used to obtain the alpha-particle count using the associated particle system. Digital data were recorded by event from the CAMAC module and analyzed offline.

In the experimental data processing, the data-taking software, Kmax, was used to obtain the initial TOF spectra of the leakage neutrons after selecting an appropriate PH threshold and neutron events via offline analysis. The initial spectra were then normalized to the neutron yields calculated based on the associated particle counts and BC-501A detector area. Hence, the final TOF spectra were in the neutron flux per unit neutron per unit area (cm^{-2}).

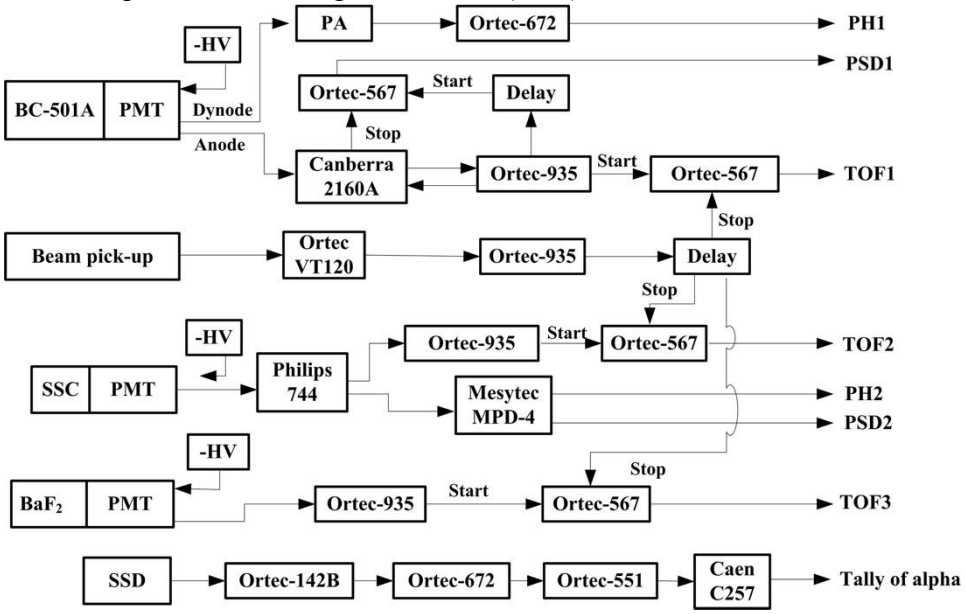

Fig.3 Block diagram of measuring circuits.

3. Monte Carlo simulation

Simulations are an essential aspect of benchmark experiments. Problems existing in the evaluated data file can be identified by comparing the measurements and predictions of different evaluated neutron libraries. The simulated TOF spectra of the leakage neutrons were calculated using MCNP-4C, in which the modeling of a 14.5 MeV source and neutron detector is crucial for obtaining accurate results.

3.1 Description of neutron source

A description of the neutron source, which primarily includes the energy, angular, and pulsed-time distributions, is shown in Fig.4. One of the calculations was performed using the TARGET[38] code, which was developed by PTB in Germany to express the energy and angular flux distributions of the neutron source. By inputting the values of the incident energy of the D^+ beam, T/Ti ratio, and T-Ti target thickness, which in this study were 300 keV, 1.8, and 1.2 mg/cm^2, respectively, a calculated distribution that could be used in the MCNP simulation was obtained. The results are presented in Fig.4a.

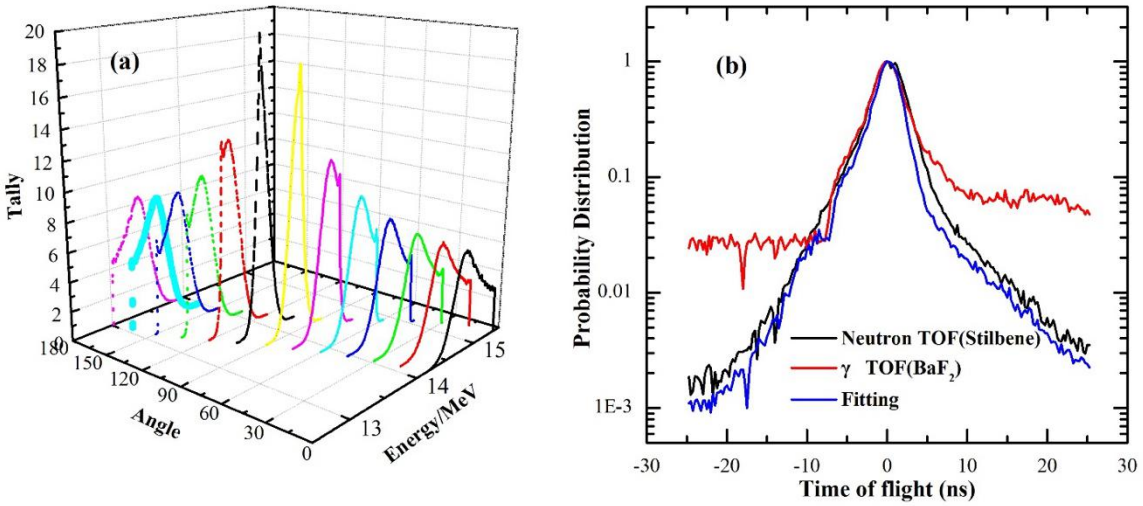

Fig.4.Description of D-T source in Monte Carlo simulation: (a) angular dependence of energy spectrum; (b) pulsed-time distribution.

The pulsed-time distribution is a critical input parameter used in the simulation of the TOF spectrum and is described by a TME card in the MCNP code. It was obtained through a fitting process of the neutron spectra from the stilbene scintillation crystal and the γ spectra from the BaF_2 scintillation detector[39]. The fitting results for the pulsed-time distribution are presented in Fig.4b.

3.2 Description of neutron detector (BC-501A)

The description of the BC-501A detector mainly includes the efficiency curve and size of the liquid scintillator detector. The efficiency of the BC-501A detector was determined by following these steps[40]. (1) The relative efficiency of BC-501A was measured using a ^{252}Cf neutron source. (2) The absolute efficiency was calibrated using a D-D neutron, and the results were used to normalize the relative efficiencies. (3) The efficiency was calculated using the NEFF code[41], and the results were validated using the experimental measurement results presented subsequently. The light output function used in the calculation was calibrated with neutrons generated via the ^{9}Be (d, n)^{10}B reaction using a 2×13 MeV Tandem accelerator at the CIAE. Fig.5 shows the shapes of the efficiency curves for different threshold values. The calculations are in good agreement with the measurements.

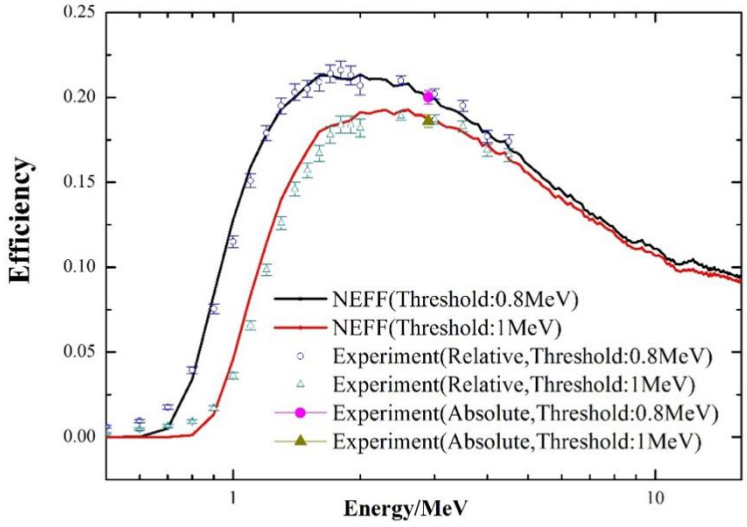

Fig.5 Detection efficiency curves of BC-501A liquid detector with different thresholds.

Detector size refers to the area and thickness of the detector. The detector can be regarded as a surface detector because its thickness was only 2.54 cm, which is significantly shorter than the flight distance of 8 m. Therefore, a ring detector estimator with a diameter of 5.08 cm was used in the MCNP-4C code.

3.3 Simulation of MCNP program

The benchmark model for the two measured angles used in the simulation is shown in Fig.6[42].When calculating the leakage neutron spectra transmitted at 60°, the material of the sample cell at 120° was described on a material card assigned to air, whereas the sample cell at 60° was assigned to air for 120° calculations. Both sample cells were assigned to air for background simulation.

The MCNP program was adopted to simulate the experiment and test the latest data of ^{238}U in CENDL-3.2, ENDF/B-VIII.0, JENDL-5.0 and JEFF-3.3, with data files of other materials, such as targets, collimators, shields, and air taken from the ENDF/B-VIII.0 library. The ACE format data suitable for the MCNP code were processed using the NJOY99 program[43]. The number of simulated histories was 10^9, making the statistical uncertainty for the calculation slower than 1% for each time bin. Based on these comparisons, it was easy to determine the differences between the four evaluated libraries.

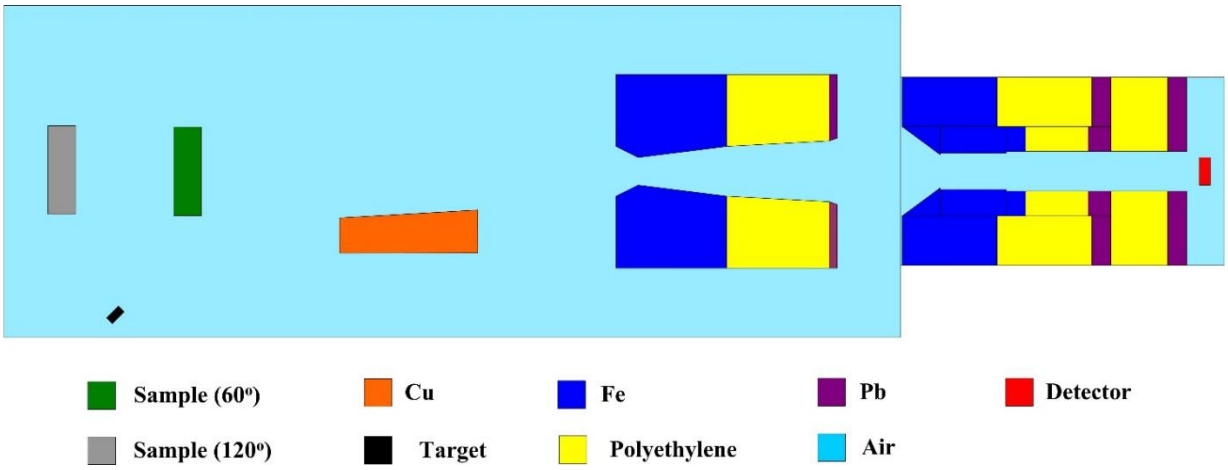

Fig.6 Geometry for MCNP simulation.

4. Results and Discussion

4.1 Experimental system test on standard samples

The leakage neutron spectra measurements on standard sample (polyethylene) with measurement angles of 45° and 60° were first conducted to verify the reliability of data acquired using this experimental system[44]. The polyethylene sample was a rectangular slab with a 30 cm square base and 6 cm thickness.

The MCNP program was used to obtain the corresponding simulated results, and the data file was obtained from the ENDF/B-VIII.0 library. The results were analyzed to examine the simulations after background deduction and return. The results are plotted in Fig.7, and the count values are listed in Table 3. The experimental results of the n-p elastic peak satisfactorily replicated the simulated results. This indicates that the processing of the experimental data is reasonable, and the system measurement data are reliable.

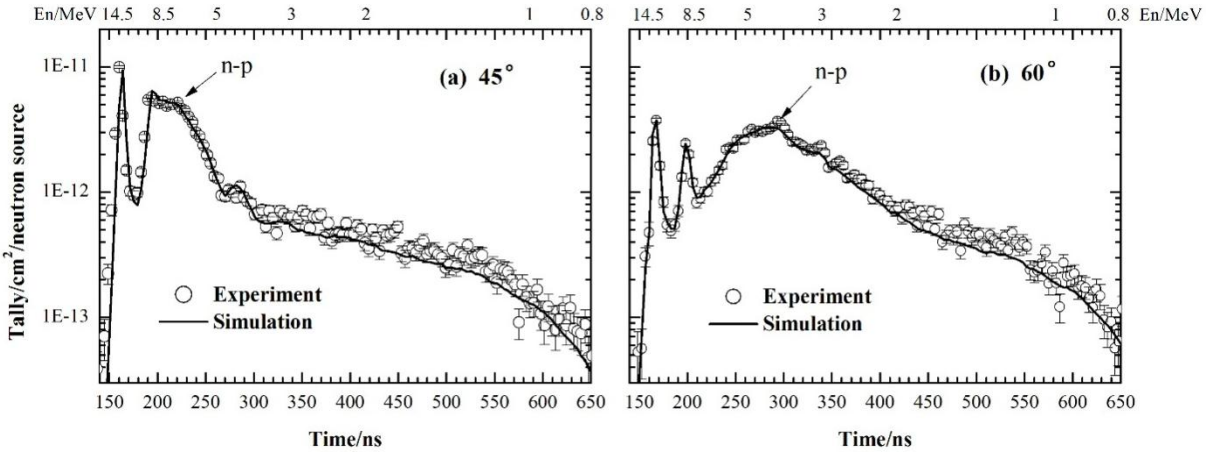

Fig.7 Comparison between calculation results for polyethylene at 45° and 60° and experimental results.

Table 3 Results for standard sample (unit source neutron and unit detector area)

Angle	Measurement	Simulation	C/E
45°	(8.42±0.28)E-11	8.25E-11	0.981±0.032
60°	(1.03±0.03)E-10	9.93E-11	0.960±0.031

4.2 Uncertainty analysis of experimental data

Normalization of the initial experimental spectra can be performed not only based on the number of associated particles, but also based on the ratio of the area of the n-p elastic peak between the experimental and simulated results. The normalized coefficient, B^1, can be determined using Eq. (5):

$$N_n = \frac{N_p^e}{N_p^c} = B^1 \times N_\alpha^p \qquad (5)$$

where N_p^e is the count of neutrons (n-p scattering) on polyethylene, N_p^c is the count of neutrons (n-p scattering) on polyethylene calculated using MCNP (unit source neutron), and N_α^p is the count of associated α on polyethylene.

The initial experimental spectra on ^{238}U sample can be normalized using Eq. (6):

$$\frac{N_U^e}{N_n} = \frac{N_U^e}{B^1 \times N_\alpha^p} = \frac{N_U^e \times N_p^c \times N_\alpha^p}{N_\alpha^U \times N_p^e} \qquad (6)$$

where N_U^e is the count of neutrons on ^{238}U (unit time bin), and N_α^U is the count of associated α on ^{238}U.

Most systematic uncertainties in ^{238}U measurements can be eliminated by normalizing the experimental data with the standard sample, as expressed by Eq. (6), which includes uncertainties in the absolute efficiency of the BC-501A detector (3%) and the ambiguity of the solid angle for associated particle detection. Finally, the total uncertainty of the experimental results consisted of the remaining systematic and statistical uncertainties. The statistical uncertainty from the neutron count from ^{238}U was better than 3% over 80% points. The others are listed in Table 4.

Table 4 Uncertainties in measurements

	source	Uncertainty (%)
Statistical	The count of neutrons (n-p scattering) on polyethylene calculated by MCNP (unit source neutron)	≤0.5
	The count of neutrons (n-p scattering) on polyethylene	≤0.5
	The count of associated α on polyethylene	≤0.5
	The count of associated α on ^{238}U	≤0.5
Systematic	The relative efficiency of neutron detection	≤3
	The ambiguity of scattering angle	≤1

4.3 Results and analysis

Leakage neutron spectra measurements were performed at 60° and 120° on slab ^{238}U using D-T neutrons. The measurements were compared with the predictions of the MCNP calculations using four evaluated neutron libraries. The comparison showed that differences existed between the simulation and measurement results. In particular, the simulation with the CENDL-3.2 library was significantly higher than the experimental results between 200 and 400 ns.

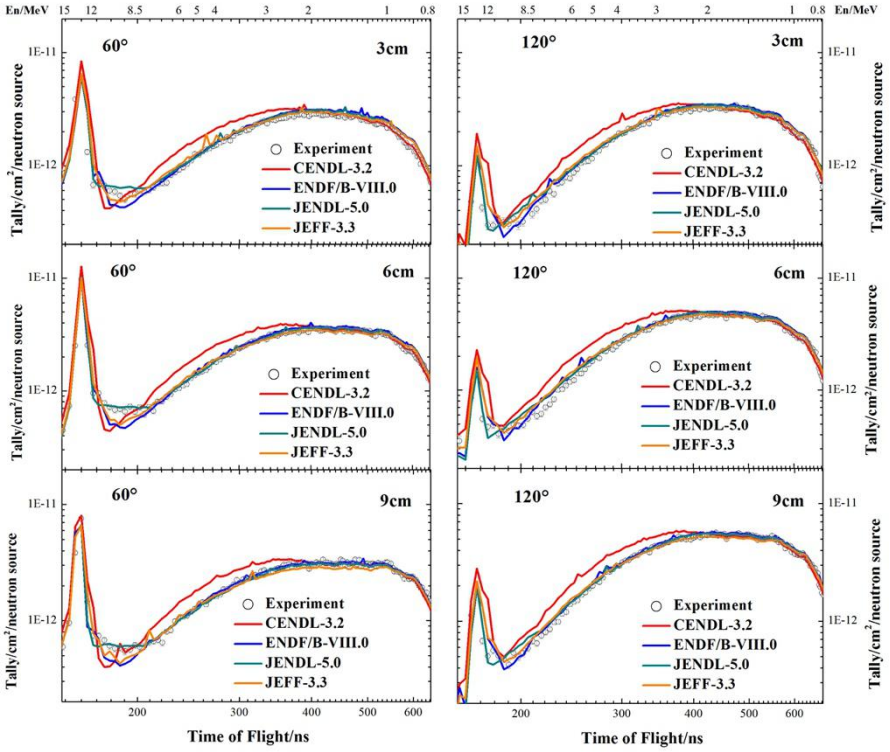

Fig.8 Comparison between calculated and measured leakage spectra on ^{238}U sample with thicknesses of 3, 6, and 9 cm at 60° and 120°.

The discrepancies between the calculated and experimental results are considered to be attributed to the reaction cross-sections associated with the production of secondary neutrons in different libraries. NDplot was used to plot the experimental and evaluated data in the neutron libraries. The ND-plot program is a simple and efficient software application for nuclear data[45]. By inputting the proton number, mass number, incident particle type, energy, and other information about the target nucleus, experimental and evaluated data, such as the reaction cross-section, secondary particle angle distribution, secondary particle energy distribution, and secondary particle energy angle distribution, can be obtained. The secondary neutrons produced through the interaction between the D-T neutrons (approximately 14.5MeV) and^{238}U are presented in Fig.9, which generally

consist of neutrons scattered via elastic and inelastic scattering, and neutrons produced through fission reactions (n, f), (n, 2n), and (n, 3n).

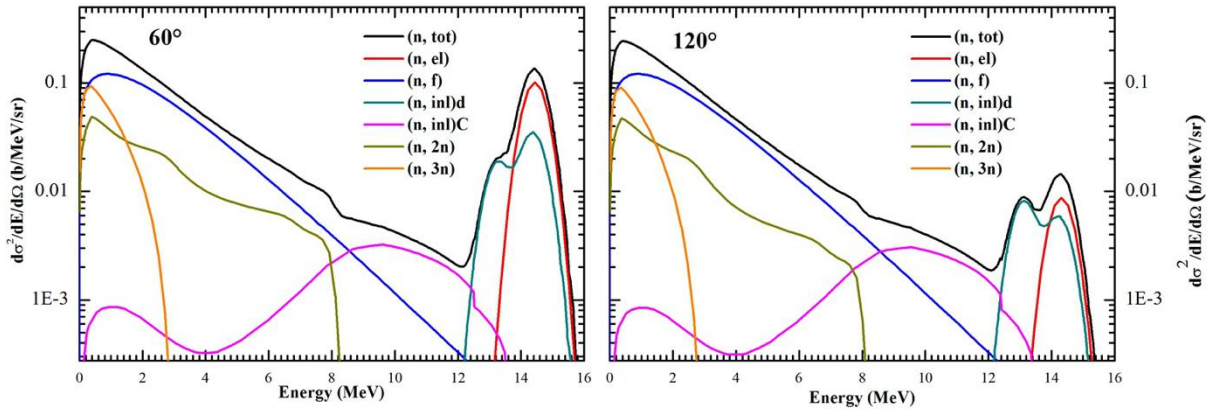

Fig.9 Energy spectra of secondary neutrons after interaction between14.5MeV neutronsand^{238}U sample at (a) 60° and (b) 120°.The data was retrieved from the CENDL-3.2 library.

Based on the different energy regions mainly contributed by different reactions, the neutron energy spectra can be divided into four energy regions: (1) 12 < E_n < 16 MeV, which consist of neutrons scattered by elastic (n, el) and inelastic discrete-level ((n, inl)d) reactions; (2) 8.5 < E_n < 12 MeV, in which the neutrons are mainly from inelastic continuum scattering ((n, inl)C) and total fission reaction (n, f); (3) 3 < E_n < 8.5 MeV, which consists of emitted neutrons from (n, f) and production of two-neutron (n,2n) reactions; (4) 0.8 < E_n < 3 MeV, which consists of emitted neutrons from (n, f), (n,2n), and (n, 3n) reactions and multiple neutron scattering.

The simulated and experimental results of the leakage neutron spectra were integrated according to the above four energy regions, and the C/E ratios of the different libraries were obtained by comparing the simulated and experimental results. The C/E ratios of the four nuclear data libraries are listed in Table 5.

Table 5 C/E ratios of leakage neutrons integrated over four energy regions for four libraries

Thickness /cm	Energy /MeV	CENDL-3.2	ENDF/B-VIII.0	JENDL-5.0	JEFF-3.3
60°					
3cm	12-16	1.385±0.046	1.006±0.033	1.020±0.034	1.081±0.036
	8.5-12	0.937±0.034	0.855±0.031	1.111±0.040	0.929±0.034
	3-8.5	1.331±0.043	1.035±0.033	1.033±0.033	1.060±0.034
	0.8-3	1.043±0.033	1.107±0.035	1.082±0.034	1.053±0.033
	0.8-16	1.123±0.036	1.080±0.034	1.069±0.034	1.054±0.033
6cm	12-16	1.378±0.044	1.030±0.033	1.030±0.033	1.094±0.035
	8.5-12	0.847±0.028	0.781±0.025	1.044±0.034	0.845±0.027
	3-8.5	1.328±0.042	1.035±0.033	1.003±0.032	1.011±0.032
	0.8-3	1.031±0.033	1.065±0.034	1.039±0.033	0.995±0.031
	0.8-16	1.105±0.035	1.052±0.033	1.031±0.032	1.001±0.032
9cm	12-16	1.297±0.043	1.032±0.034	1.000±0.033	1.051±0.035
	8.5-12	0.913±0.033	0.791±0.029	1.016±0.037	0.839±0.031
	3-8.5	1.313±0.042	1.015±0.032	0.973±0.031	0.981±0.031
	0.8-3	1.001±0.032	1.012±0.032	0.983±0.031	0.933±0.030
	0.8-16	1.076±0.034	1.010±0.032	0.982±0.031	0.947±0.030
120°					
3cm	12-16	1.909±0.089	1.203±0.056	1.026±0.048	1.384±0.063
	8.5-12	1.278±0.051	0.968±0.039	1.171±0.047	1.099±0.044

	3-8.5	1.331±0.042	1.038±0.033	1.030±0.033	1.064±0.034
	0.8-3	1.003±0.032	1.066±0.034	1.048±0.033	1.014±0.032
	0.8-16	1.082±0.034	1.061±0.034	1.045±0.033	1.029±0.033
	12-16	1.828±0.076	1.195±0.050	1.004±0.042	1.351±0.056
	8.5-12	1.326±0.049	1.018±0.038	1.165±0.043	1.108±0.041
6cm	3-8.5	1.355±0.043	1.064±0.034	1.049±0.033	1.054±0.034
	0.8-3	1.013±0.032	1.057±0.033	1.038±0.033	0.999±0.032
	0.8-16	1.093±0.035	1.059±0.034	1.042±0.033	1.014±0.032
	12-16	1.853±0.073	1.183±0.047	1.017±0.040	1.295±0.051
	8.5-12	1.275±0.047	1.043±0.038	1.149±0.042	1.067±0.039
9cm	3-8.5	1.328±0.042	1.045±0.033	1.013±0.032	1.016±0.032
	0.8-3	1.010±0.032	1.042±0.033	1.023±0.032	0.977±0.031
	0.8-16	1.078±0.034	1.044±0.033	1.022±0.032	0.989±0.031

Based on the C/E ratios, some deviations were observed between the simulated and experimental results.

(1) In the $12 < E_n < 16$ MeV region, the neutrons from elastic scattering were predominant at 60°, whereas at 120°, the neutrons from inelastic discrete-level scattering were predominant. The simulations with CENDL-3.2 yielded considerable overestimations in both directions, particularly in the direction of 120°, which reached approximately 80%. The simulations with JEFF-3.3 and ENDF/B-VIII.0 satisfactorily reproduced the measurements at 60°; however, in the direction of 120°, overestimations of approximately 20% and 30% were obtained, respectively. The simulations with JENDL-5.0 accurately predicted the experimental values at both angles.

The angular distributions of secondary neutrons from (n, el) and (n, inl)d reactions after the interaction of the 14.5-MeV neutron with the ^{238}U sample are shown in Fig.10a and 10b, respectively, and the cross-sections of different libraries at 60° and 120° are listed in Table 6.The (n, el) and (n, inl)d cross-sections at 14.5 MeV in the CENDL-3.2 file are larger than those from the other three libraries at both angles. In particular, the data for the (n, el) reaction reaches 7.86E-03 b at 120°, which is significantly higher than that in the JENDL-5.0 file (2.50E-03 b). The larger (n, inl)d cross-section (9.42E-03 b) in the ENDF/B-VIII.0 file results in the overestimation of the calculations at 120° in this region. The overestimation of the calculations with the JEFF-3.3 file at 120° is principally because of the larger (n, el) cross-section (3.51E-03 b) in it.

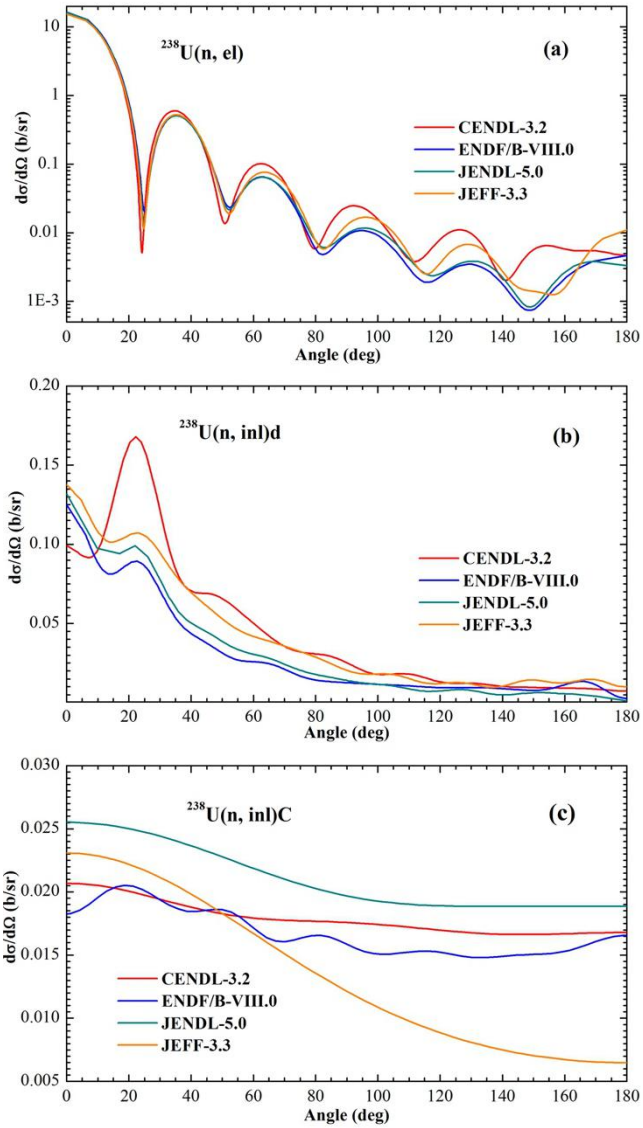

Fig. 10 Angular distribution of secondary neutron from different reactions for ^{238}U at 14.5 MeV, retrieved from four data files: (a) elastic scattering (n, el), (b) inelastic discrete-level scattering (n, inl)d, and (c)inelastic continuum scattering (n, inl)C.

Table 6 (n, el) and (n,inl)d reaction cross-sections for ^{238}U at 14.5 MeV obtained from four different data files (unit:b)

library	degree	(n, el)	(n, inl)d	(n, el) + (n, inl)d
CENDL-3.2	60	9.35E-02	5.05E-02	1.44E-01
	120	7.86E-03	1.32E-02	2.10E-02
ENDF/B-VIII.0	60	5.92E-02	2.58E-02	8.50E-02
	120	2.24E-03	9.42E-03	1.17E-02
JENDL-5.0	60	5.85E-02	3.05E-02	8.90E-02
	120	2.50E-03	7.25E-03	9.75E-03
JEFF-3.3	60	6.52E-02	4.20E-02	1.07E-01
	120	3.51E-03	1.20E-02	1.55E-02

(2) In the $8.5 < E_n < 12$ MeV region, the simulations with the CENDL-3.2 file showed a good agreement with the measured spectra at 60° but yielded an overestimation of approximately 30% at 120°. However, the simulations with ENDF /B-VIII.0 was consistent with the measurements at 120° but yielded an underestimation of approximately 20% at 60°. The calculations with the JENDL-5.0 file somewhat replicated the measured spectra at 60° but gave a slight overestimation at 120°. The calculations with the JEFF-3.3 files lightly underestimated the measurements at 60° but accurately predicted the measurement results at 120°.

The angular and energy distributions of secondary neutrons from the (n, inl)C reaction after the interaction of the 14.5-MeV neutron with ^{238}U are shown in Figs.10c and 11a. The angular distribution and energy spectrum provided by the CENDL-3.2 file at 120° were lower than those of JENDL-5.0, but the calculations using CENDL-3.2 appeared to overestimate the production of neutrons more than the JENDL-5.0 calculations. This effect mainly resulted from the contribution by neutrons partly scattered by the (n, el) reaction in the 8.5–12 MeV energy region owing to the wider width of the pulsed beam from the measurements. The angular distribution of the secondary neutrons at 120° obtained by the CENDL-3.2 file was higher than those of the other libraries (Fig.10a).

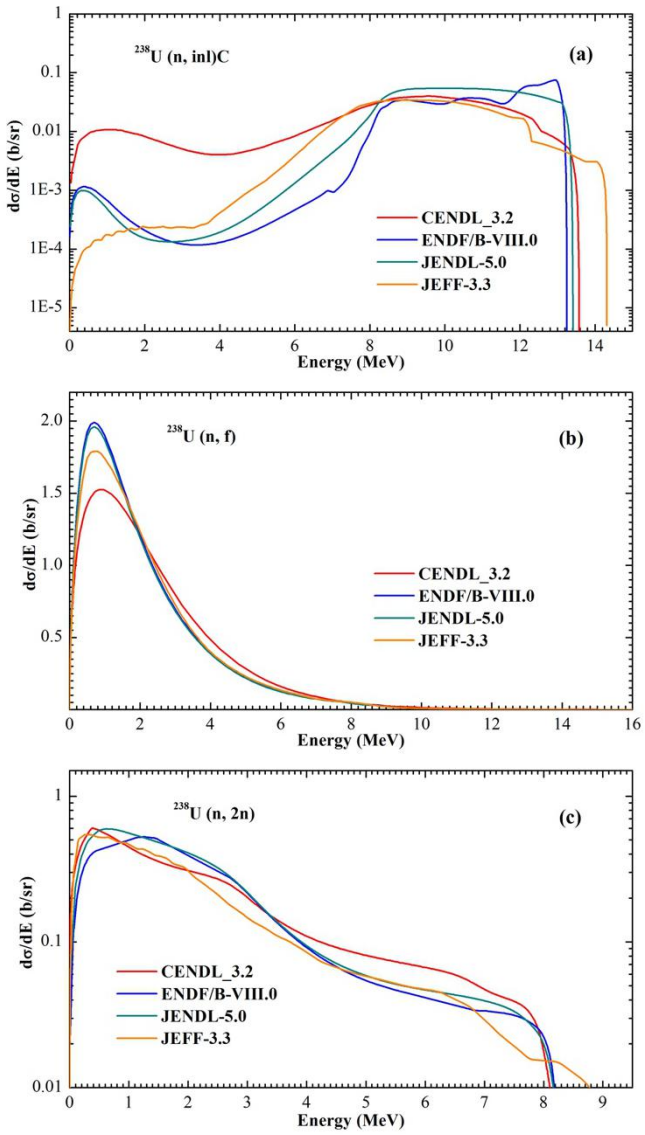

Fig. 11 Energy spectra of secondary neutrons from several reaction channels for ^{238}U at 14.5 MeV, retrieved from four data files: (a) continuous-level elastic scattering (n ,inl)C, (b) fission reaction (n, f), and (c) (n, 2n) reaction.

(3) In the $3.0 < E_n < 8.5$ MeV region, the simulations with ENDF/B-VIII.0, JENDL-5.0, and JEFF-3.3 libraries show good agreements with the measured leakage spectra. However, the results obtained with CENDL-3.2 significantly overestimated the measurement results at both 60° and 120°. The discrepancy between the measured spectrum and that calculated with the CENDL-3.2 file is mainly because the energy distributions of secondary neutrons from fission and the (n, 2n) reactions are harder than those in the other three libraries. As shown in Figs.11b and 11c, the shape of the energy spectrum of secondary neutrons from the fission reaction in CENDL-3.2was higher than those from other files in the 3–8 MeV energy interval but lower in the 0.8–3 MeV interval. Moreover, the spectrum from the (n, 2n) reaction in CENDL-3.2 was higher than those from other files in the 3.5–8 MeV interval but lower in the 1–3.5 MeV region.

(4) In the $0.8 < E_n < 3.0$ MeV region, calculations performed using the four libraries accurately predicted the measurement results.

(5) Across the entire energy region (0.8–16 MeV), the calculation values obtained with the CENDL-3.2 file were slightly higher than the measurement values, and the C/E ratios were closer to 1 with an increase in sample thickness.

A comparison between the measured spectra and those calculated with the CENDL-3.2 and JENDL-5.0 files was performed at each time bin, and the C/E ratios were plotted (Fig. 12). The C/E ratios of the leakage spectra calculated with the CENDL-3.2 file to the measured spectra tended to deviate from 1 over the high-energy region; however, the ratios became closer to 1with decreasing energy. The C/E ratios of the spectra calculated with the JENDL-5.0 file to the measured spectra are generally very close to 1 in most energy regions, except for those that are slightly higher than 1 at approximately 10 MeV.

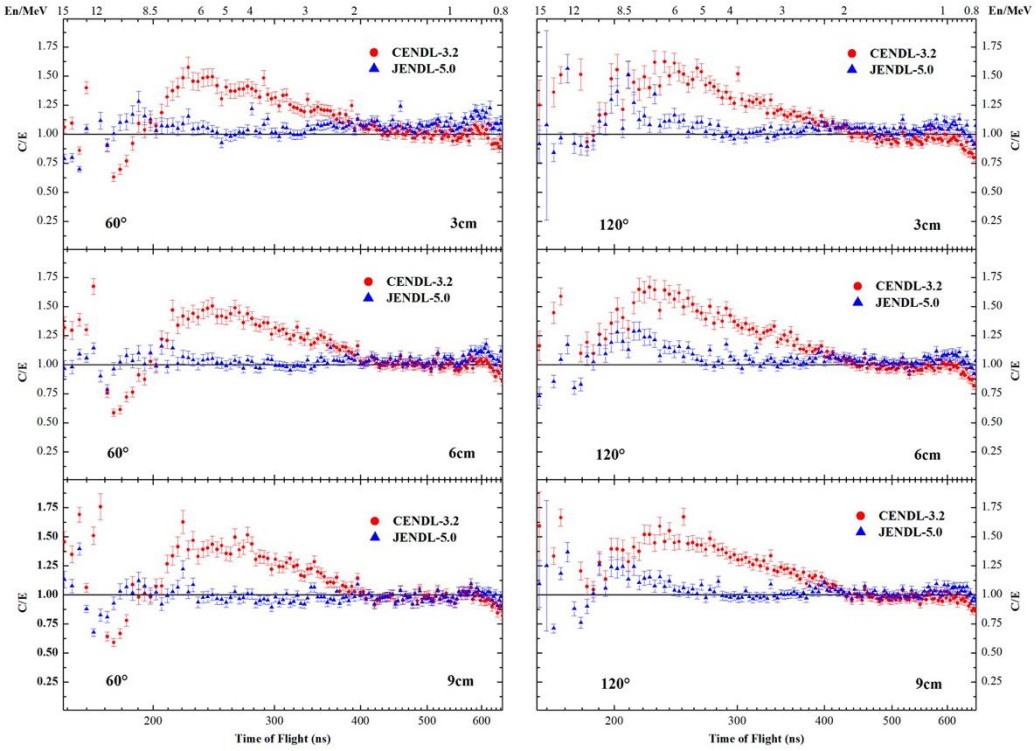

Fig. 12 C/E ratios for leakage neutrons leaking from ^{238}U with transport calculations obtained usingCENDL-3.2 and JENDL-5.0 evaluated data files.

5. Summary

An integral benchmark experiment on a rectangular-slab ^{238}U sample irradiated from a D-T neutron source was conducted to test the evaluated nuclear data. The leakage neutron spectra measurements were conducted at 60° and 120° using the TOF technique. The experimental results of the neutron TOF spectra were analyzed via Monte Carlo calculations, which were performed using ^{238}U nuclear data collected from CENDL-3.2, ENDF/B-VIII.0, JENDL-5.0, and JEFF-3.3 files. The measured and calculated spectra were compared based on the shape of the leakage spectra and the C/E ratios integrated over five different energy regions. The calculations with the JENDL-5.0 file satisfactorily predicted the experimental results; however, the calculations with CENDL-3.2 overestimated or underestimated the measurements in different energy regions. These discrepancies were caused by the inaccurate angular or energy distribution of secondary neutrons in the evaluated data file. In summary, the angular distribution of secondary neutrons from the (n, el) reaction and the

energy distribution of secondary neutrons from the (n, inl) and (n, fission) reactions in ^{238}U in the CENDL-3.2 library should be improved in future studies.

Acknowledgments

The authors acknowledge all their colleagues in the accelerator operating group at CIAE for providing excellent experimental conditions. This study was supported by the general program (Grant No. 1177531) and joint funding (Grant No. U2067205) from the National Natural Science Foundation of China.

References

1 C. Wulandari, A. Waris, S. Permana et al., Evaluating the JEFF 3.1, ENDF/B-VII.0, JENDL 3.3, and JENDL 4.0 nuclear data libraries for a small 100 MWe molten salt reactor with plutonium fuel. Nucl. Sci. Tech. **33**, 165 (2022). https://doi.org/10.1007/s41365-022-01141-8

2 Z. Z. Ren, Y.W. Yang, Y.H. Chen et al., Measurement of the $^{232}Th(n,f)$ cross section in the 1–200 MeV range at the CSNS Back-n. Nucl. Sci Tech. **34**, 115 (2023). https://doi.org/10.1007/s41365-023-01271-7

3 X. Li, L. Liu, W. Jiang et al., Experimental determination of the neutron resonance peak of 162Er at 67.8 eV. PHYS. REV. C **106**, 065804 (2022). https://doi.org/10.1103/PhysRevC.106.065804

4 G.L. Wang, H.Y. Lan, X.M. Shi et al., A general framework for describing photofission observables of actinides at an average excitation energy below 30 MeV*. Chin. Phys. C **46**, 084102 (2022). doi: 10.1088/1674-1137/ac6abc

5 Z.G. Ma, H.Y. Lan, W.Y. Liu et al., Photonuclear production of medical isotopes 62,64Cu using intense laser-plasma electron source. Matter Radiat. Extrem. **4**, 064401 (2019). https://doi.org/10.1063/1.5100925

6 C. L. Lan, B. L. Xie, K. Zhang et al., Measurement of $^{232}Th(n,2n)^{231}Th$ reaction cross sections at neutron energies of 14.1 MeV and 14.8 MeV using neutron activation method. Nucl. Sci. Tech. **26**, 060501 (2015). Doi:10.13538/j.1001-8042/nst.26.060501

7 B. Zhang, X. B. Ma, K. Hu et al., Performance of the CENDL-3.2 and other major neutron data libraries for criticality calculations. Nucl. Sci. Tech. **33**, 8 (2022). doi:10.1007/s41365-022-00994-3

8 Y. Oyama, H. Maekawa, Measurement and analysis of an angular neutron flux on a beryllium slab irradiated with Deuterium-Tritium neutrons. Nucl. Sci. Eng. **97**, 220-234 (1987). https://doi.org/10.13182/NSE87-A23504

9 I. Murata, T. Nishio, T. Kokooo et al., Benchmark experiment on $LiAlO_2$, Li_2TiO3 and Li_2ZrO_3 assemblies with D-T neutrons-leakage neutron spectrum measurement. Fusion Eng. Des. **51-52**, 821-827 (2000). https://doi.org/10.1016/S0920-3796(00)00200-3

10 D. V. Markovskij, A. I. Blokhin, V.A. Chirkin et al., Integral benchmark experiments with 14 MeV neutrons for testing the nuclear data of vanadium. Fusion Eng. Des. **69**, 419-423 (2003). https://doi.org/10.1016/S0920-3796(03)00084-X

11 J. P. Freidberg, A. C. Kadak, Fusion-fission hybrids revisited. Nat. Phys. **5**, 370-372 (2009). http://dx.doi.org/10.1038/nphys1288

12 R. Liu, T.H. Zhu, X.S. Yan et al., Reaction rates in blanket assemblies of a fusion-fission hybrid reactor. Nucl. Sci. Tech. **23**, 242-246(2012). doi: 10.13538/j.1001-8042/nst.23.242-246

13 C. D. Bowman, E. D. Arthur, P. W. Lisowski et al., Nuclear energy generation and waste transmutation using an accelerator-driven intense thermal neutron source. Nucl. Instrum. Meth. A **320**, 336-367 (1992). http://dx.doi.org/10.1016/0168-9002(92)90795-6
14 Z. Q. Chen, Recent progress in nuclear data measurement for ADS at IMP. Nucl. Sci. Tech. **28**, 184 (2017). https://doi.org/10.1007/s41365-017-0335-3
15 A. Degtyarev, A. Myasnikov, L. Ponomarev, Molten salt fast reactor with U-Pu fuel cycle. Prog. Nucl. Energy**82**, 33-36 (2015). http://dx.doi.org/10.1016/j.pnucene.2014.07.014
16 A.M. Daskalakis, R.M. Bahran, E.J. Blain et al., Quasi-differential neutron scattering from ^{238}U from 0.5 to 20MeV. Ann. Nucl. Energy **73**, 455-464 (2014). http://dx.doi.org/10.1016/j.anucene.2014.07.023
17 R. Capote, A. Trkov, M. Sin et al., Physics of neutron interactions with ^{238}U: New developments and challenges. Nucl. Data Sheets **118**, 26–31 (2014). https://doi.org/10.1016/j.nds.2014.04.003
18 M.B. Chadwick, E. Dupont, E. Bauge et al., The CIELO Collaboration: Neutron Reactions on ^{1}H,^{16}O,^{56}Fe, ^{235,238}U, and ^{239}Pu. Nucl. Data Sheets **118**, 1-25 (2014). http://dx.doi.org/10.1016/j.nds.2014.04.002
19 A. Plompen, T. Kawano, R. Capote, Summary Report of Technical Meeting on Inelastic Scattering and Capture Cross-section Data of Major Actinides in the Fast Neutron Region (INDC(NDS)--0597).http://www-nds.iaea.org/publications/indc/indc-nds-0597.pdf
20 Z. G. Ge, R. R. Xu, H. C. Wu et al., CENDL-3.2: The new version of Chinese general purpose evaluated nuclear data library. EPJ Web Conf. **239**, 09001 (2020). https://doi.org/10.1051/epjconf/202023909001
21 D.A. Brown, M.B. Chadwick, R. Capote et al., ENDF/B-VIII.0: The 8th Major Release of the Nuclear Reaction Data Library with CIELO-project Cross Sections, New Standards and Thermal Scattering Data. Nucl. Data sheets **148**, 1-142 (2018). https://doi.org/10.1016/j.nds.2018.02.001
22 O. Iwamoto, N. Iwamoto, S. Kunieda et al., Japanese evaluated nuclear data library version 5: JENDL-5. J. Nucl. Sci. Technol. **60**, 1-60 (2023). https://doi.org/10.1080/00223131.2022.2141903
23 O. Cabellos, F. Alvarez -Velarde, M. Angelone et al., Benchmarking and validation activities within JEFF project. EPJ Web Conf. **146**, 06004 (2017). https://doi.org/10.1051/epjconf/201714606004
24 J. S. Zhang, User manual of FUNF code for fissile material data calculation. Technical Report, CNIC-01782, cndc-0037, China, Mar 15,2006.
25 B.V. Carlson, The optical model and ECIS95,*Conference: workshop on nuclear reaction data and nuclear reactors: Physics, design and safety*, Trieste (Italy), 15 Apr - 17 May 1996.
26 P. D. Kunz, E. Rost, The distorted-wave born approximation, Computational Nuclear Physics 2, edited by K. Langanke et al. (Spinger-Verlag, New York,1993), p. 88-107
27 L. F. Hansen, C. Wong, T. T. Komoto et al., Neutron and gamma-ray spectra from ^{232}Th,^{235}U,^{238}U, and ^{239}Pu after bombardment with 14-MeV neutrons. Nucl. Sci. Eng. **72**, 35-51 (1979). https://doi.org/10.13182/NSE79-A19307
28 Y.B. Nie, J.C. Bao, X. Ruan et al., Benchmarking of evaluated nuclear data for uranium by a 14.8MeV neutron leakage spectra experiment with slab sample. Ann. Nucl. Energy **37**, 1456-1460 (2010). https://doi.org/10.1016/j.anucene.2010.06.018
29 Q. Sun, Z. Chen, R. Han et al., Experiment on uranium slabs of different thicknesses with D-T neutrons and validation of evaluated nuclear data. Fusion Eng. Des. **125**, 9-17 (2017). http://dx.doi.org/10.1016/j.fusengdes.2017.10.021

30 J. Briesmeister (Ed.), MCNP – a general Monte Carlo N-Particle transport code system, Version 4C, Report LA-13709-M, 2000.
31 Y. Nie, J. Ren, X. Ruan et al., Benchmarking of evaluated nuclear data for iron by a TOF experiment with slab samples. Fusion Eng. Des. **145**, 40-45 (2019). https://doi.org/10.1016/j.fusengdes.2019.05.021
32 S. Zhang, Y.B. Nie, J. Ren et al., Benchmarking of JEFF-3.2, FENDL-3.0 and TENDL-2014 evaluated data for tungsten with 14.8 MeV neutrons. Nucl. Sci. Tech. **28**, 27 (2017). https://doi.org/10.1007/s41365-017-0192-0
33 Y. Ding, Y. Nie, J. Ren et al., Benchmark experiment for bismuth by slab samples with D-T neutron source. Fusion Eng. Des. **167**, 112312 (2021). https://doi.org/10.1016/j.fusengdes.2021.112312
34 Y.Y. Ding, Y.B. Nie, J. Ren et al., The benchmark experiment on slab iron with D-T neutrons for validation of evaluated nuclear data. Ann. Nucl. Energy **132**, 236-242 (2019). https://doi.org/10.1016/j.anucene.2019.04.041
35 Q. P. Zhong, X. J. Chen, H. L. Lu et al., Background Analysis for an Associated Particle Method to Measure the Neutron Fluence Rate From the T(d,n)^{4}He Neutron Source. Atomic Energy Science and Technology**39**, 131-133 (2005). doi: 10.7538/yzk.2005.39.02.0130 (in Chinese)
36 T. H. Zhu, R. Liu, L. Jiang et al., The associated proton monitoring technique study of D-D source neutron yields at the large angle. Nuclear Electronics & Detection Technology**27**, 141-145 (2007) (in Chinese)
37 X. G. Cai, Y. B. Nie, J. Bao et al., Design of a pre-collimator system for neutronics benchmark experiment[J]. NUCLEAR TECHNIQUES**36**, 010201 (2013).doi: 10.11889/j.0253-3219.2013.hjs.36.010201 (in Chinese)
38 D. Schlegel, TARGET User's Manual, Physikalisch-Technische Bundesanstalt, Braunschweig, Germany, 2005.
39 Y.B. Nie, J. Ren, X.C. Ruan et al., Benchmark experiments with slab sample using time-of-flight technique at CIAE. Ann. Nucl. Energy **136**, 107040 (2020). https://doi.org/10.1016/j.anucene.2019.107040
40 J. Ren, Y. B. Nie, X. C. Ruan et al., Calibration of Neutron Detection Efficiency for Liquid Scintillator with ^{252}Cf Fission Gamma Ray and Time-of-Flight Method. Atomic Energy Science and Technology **2**, 215-220 (2018). doi: 10.7538/yzk.2017.youxian.0258(in Chinese)
41 G. Dietze, H. Klein, NRESP4 and NEFF4 Monte Carlo Code for the Calculation of Neutron Response Functions and Detection Efficiencies for NE213 Scintillation Detectors.
42 Y. Ding, Y. Nie, J. Ren et al., Measurement and Simulation of Neutron Leakage Spectrum with Different Sized Polyethylene Samples. Atomic Energy Science and Technology**51**, 223-229 (2017).doi: 10.7538/yzk.2017.51.02.0223 (in Chinese)
43 R. E. Macfarane, D.W. Muri, R. M. Boicourt et.al., The NJOY Nuclear Data Processing System, Version 6, LA-UR-17-20093, Los Alamos National Laboratory, December, 2016.
44 K. Zhang, Y.B. Nie, J. Bao et al., Verification of the integral experimental system with standard sample method. NUCLEAR TECHNIQUES **37**, 080501 (2014). doi: 10.11889/j.0253-3219.2014.hjs.37.080501 (in Chinese)
45 Y. L. Jin, X. Tao, J. M. Wang et al., NDplot – A plotting tool for nuclear data. EPJ Web of Conf. **239**, 10004 (2020). https://doi.org/10.1051/epjconf/202023910004